Femtosecond X-Ray Diffraction: Experiments and Limits

J.S. Wark,[a] A.M. Allen,[a] P.C. Ansbro,[a] P.H. Bucksbaum,[b] Z. Chang,[b] M. DeCamp,[b] R.W. Falcone,[c] P.A. Heimann,[d] S.L. Johnson,[c] I. Kang,[c] H.C. Kapteyn,[b] J. Larsson,[e] R.W. Lee,[f] A.M. Lindenberg,[c] R. Merlin,[b] T. Missalla,[e] G. Naylor,[g] H.A. Padmore,[d] D.A. Reis,[b], K. Scheidt,[g] A. Sjoegren,[e] P.C. Sondhauss[a] and M. Wulff[g]

[a]Department of Physics, Clarendon Laboratory, University of Oxford Parks Road, Oxford, OX1 3PU UK

[b]Department of Physics, The University of Michigan, Ann Arbor, MI 48109 USA

[c]Department of Physics, University of California, Berkeley, CA 94720 USA

[d]Advance Light Source, Lawrence Berkeley National Laboratory, Berkeley, CA 94720 USA

[e]Atomic Physics Division, Lund Institute of Technology, Lund Sweden

[f]Lawrence Livermore National Laboratory, Livermore, CA 94551 USA

[g]European Synchrotron Radiation Facility, Grenoble 38043 France

ABSTRACT

Although the realisation of femtosecond X-ray free electron laser (FEL) X-ray pulses is still some time away, X-ray diffraction experiments within the sub-picosecond domain are already being performed using both synchrotron and laser-plasma based X-ray sources. Within this paper we summarise the current status of some of these experiments which, to date, have mainly concentrated on observing non-thermal melt and coherent phonons in laser-irradiated semiconductors. Furthermore, with the advent of FEL sources, X-ray pulse lengths may soon be sufficiently short that the finite response time of monochromators may themselves place fundamental limits on achievable temporal resolution. A brief review of time-dependent X-ray diffraction relevant to such effects is presented.

Keywords: Femtosecond Diffraction, Coherent Phonons, Time-Resolved Diffraction

1. INTRODUCTION

The development of high-brightness sub-picosecond X-ray sources offers the potential for a variety of novel experiments in both the life and physical sciences.[1–8] Whilst it is clear that several of the intended performance characteristics of X-ray FELs are far superior to the sources of the present, it should nevertheless be noted that experiments of significance are already being performed with extant technology. Resolution of, or better than 1-picosecond can be obtained with both laser-based and synchrotron sources. In the field of material science, emphasis to date has been made on the study of coherent acoustic phonons,[5,6] and the phenomenon of non-thermal melting.[7,8] Experiments demonstrating diffraction from coherent optical phonons have also been proposed.[9] In this paper we briefly summarise the developments in the study of coherent phonons, and note that the novel FEL sources promise the superior temporal resolution that may well be required to interrogate several relevant effects.

The paper is arranged in the following manner. We first present the underlying theory of time-resolved X-ray diffraction from coherent phonons, be they acoustic or optical, propagating in otherwise perfect single crystals. We then describe experiments that have been performed to observe coherent acoustic phonons, and compare the experimental results with simulations. Preliminary simulations of diffraction from coherent optical phonons are then presented, and an introduction to the Phonon-Bragg switch[9] based on optical phonons given. We conclude with a discussion of the conditions under which full time-dependence needs to be retained within the diffraction simulations, and prospects for FEL-based experiments in this area.

Correspondence: E-mail:justin.wark@physics.ox.ac.uk

X-Ray FEL Optics and Instrumentation, Dennis M. Mills, Horst Schulte-Schrepping, John R. Arthur, Editors, Proceedings of SPIE Vol. 4143 (2001) © 2001 SPIE · 0277-786X/01/$15.00

2. TIME-DEPENDENT X-RAY DIFFRACTION

The theory of X-ray diffraction from perfect crystals has been developed by a number of authors over several years: we refer the reader to the classic text by Zachariasen for an elegant treatment of this well-known phenomenon.[10] The description we provide here, developed independently by several authors,[11–14] is identical to the classical theory save for the fact that we explicitly keep the time-dependence of the incident and diffracted radiation. As such the theory is still valid in the case where the X-ray properties of the crystal alter on a time-scale less than or comparable with the time taken for an X-ray to traverse an extinction depth - which could be several tens or even hundreds of femtoseconds for weak reflections in large perfect crystals.

Following the normal dynamical theory, we take the susceptibility of the crystal to be complex and periodic (we discuss the specific modifications introduced by coherent phonons at a later stage). However, we also allow the Fourier components of the susceptibility to be functions of both time and position within the crystal, as we now assume that the electron density is both time and space dependent. This is a reasonable description of the crystal if the scalelengths of the susceptibility are long compared with an interatomic spacing. Such an approach can, for example, deal with a relatively long-wavelength but high frequency optical phonon. Thus the susceptibility can be represented by a Fourier series:

$$\psi(\mathbf{r},t) = \sum_H \psi_H(\mathbf{r},t)\exp(-i\mathbf{G_H}\cdot\mathbf{r}) \tag{1}$$

where $\mathbf{G_H}$ is the reciprocal lattice vector associated with the planes H, where $H \equiv (h,k,l)$, and h,k,l are the Miller indices. We denote the real and imaginary parts of $\psi_H(\mathbf{r},t)$ by

$$\psi_H(\mathbf{r},t) = \psi_H^{'}(\mathbf{r},t) + i\psi_H^{''}(\mathbf{r},t) \tag{2}$$

In our analysis we will assume that the timescales of the changes in the susceptibility of the crystal, and the electric field associated with the X-ray pulse are long compared with the period of the X-ray pulse. That is to say we take the first order approximation, and assume that the magnitude of terms is such that

$$\frac{\partial\psi(\mathbf{r},t)}{\partial t}\mathbf{E} \ll \frac{\partial\mathbf{E}}{\partial t} \tag{3}$$

where $\mathbf{E}$ is the electric field of the X-ray. This approximation is justified due to the small value of ψ for X-rays, and considering that the suspectibility and X-ray amplitude vary on similar timescales. The form given to the incident wave in the vacuum is

$$\mathbf{D}(\mathbf{r},t) = \mathbf{D_0}(\mathbf{r},t)\exp[i(\omega_o t - \mathbf{k_0}\cdot\mathbf{r})] \tag{4}$$

where ω_0 remains constant in the vacuum and the crystal. In the vacuum, $\mathbf{D_0}(\mathbf{r},t)$ is taken to be real but time and space dependent; within the crystal the incident wave is also given by equation (4), in this case $\mathbf{k_0}$ is kept constant and the perturbations to the phase and amplitude of the wave introduced by the crystal are introduced into $\mathbf{D_0}(\mathbf{r},t)$, and thus it becomes complex (note that for X-rays $\psi \sim 10^{-4}$). The wave is reflected from the H-planes, and within the crystal is given by

$$\mathbf{D}(\mathbf{r},t) = \sum_H \mathbf{D_H}(\mathbf{r},t)\exp[i(\omega_o t - (\mathbf{k_0}+\mathbf{G_H})\cdot\mathbf{r}] \tag{5}$$

This equation can be generalised to include the incident wave by allowing H to take the value $(0,0,0)$ with the convention that $\mathbf{G_0}\cdot\mathbf{r} \equiv 0$.

With these assumptions we find that the time dependent dynamical diffraction equations reduce to those found previously in the standard dynamical theory, save that the Fourier components of the susceptibility are now themselves functions of both time and position, and the derivative with respect to time of the envelope of the wave field must be considered explicitly. That is to say that when we equate terms in the incident and diffracted directions and take the first order approximation we find:

$$i\frac{\lambda\partial D_0}{\pi\partial x_0} = \psi_0 D_0 + \psi_H D_H - i\frac{\lambda\partial D_0}{c\pi\partial t} \tag{6}$$

$$i\frac{\lambda\partial D_H}{\pi\partial x_H} = \psi_0 D_H + \psi_H D_0 - \alpha_H D_H - i\frac{\lambda\partial D_H}{c\pi\partial t} \tag{7}$$

where α_H is a quantitity that represents the deviation from the Bragg angle and, for a perfect crystal, is given by

$$\alpha_H = \frac{\mathbf{G_H}^2 + 2\mathbf{G_H}\cdot\mathbf{k_0}}{\mathbf{k_0}^2} \equiv -2(\theta - \theta_B)\sin(2\theta_B) \tag{8}$$

It is the solution to equations (6) and (7) that we seek. Given the boundary conditions that we know the value of the incident amplitude at the surface of the crystal, we solve for the reflected amplitude (and hence intensity) at the exit surface. In the absence of explicit time-dependence, rapid solutions based on analytic solutions in the lamina approximation exist.[15]

As alluded to above, the derivative with respect to time need only be included explicity if the crystal properties alter on a timescale comparable with the time taken for an X-ray to traverse an extinction depth. Current experiments observing coherent acoustic phonons have observed changes on the picosecond timescale, and it is the study of optical phonons (with frequencies of several Terahertz) and non-thermal melting (thought to occur on time-scales less than 100 fs) where such terms may conceivably be important.

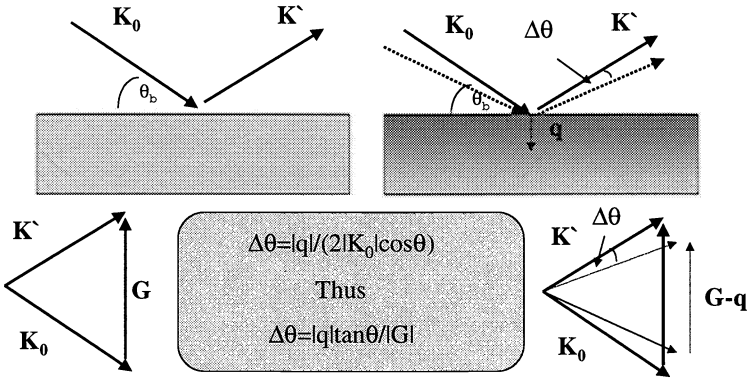

Fig. 1. Diffraction of an incident X-ray of wavevector $\mathbf{k_0}$ into a ray of wavevector $\mathbf{k}'$ from a plane with reciprocal lattice vector $\mathbf{G_H}$ in the (a) absence and (b) presence of a coherent phonon of wavevector $\mathbf{q}$.

2.1. DIFFRACTION FROM COHERENT PHONONS

Coherent phonons, be they acoustic or optical, introduce an additional periodicity into the crystal. Before outlining how such phonons can be included in an approximate manner within the dynamical theory, we note that we might expect to observe diffracted radiation at angles other than the original Bragg angle simply from wavevector matching considerations. Fig. 1(a) illustrates in schematic form the diffraction of an incident X-ray of wavevector $\mathbf{k_0}$ into a wave of wavevector $\mathbf{k}'$ from a plane with reciprocal lattice vector $\mathbf{G_H}$. The normal Bragg condition is given by $2\mathbf{k_0}\cdot\mathbf{G_H} = \mathbf{G_H}^2$, i.e. $\mathbf{k_0} + \mathbf{G_H} = \mathbf{k}'$. However, if we assume coherent phonons of wavevector $\mathbf{q}$ exist within the crystal, then we might expect the Bragg condition to be met when $\mathbf{k_0} + \mathbf{G_H} \pm \mathbf{q} = \mathbf{k}'$ as shown in Fig. 1(b). Thus diffraction will occur at angles other than the original Bragg angle. We note that in principle modulations in the susceptibility imply that more than one incident and diffracted ray may exist within the body of the crystal. Such additional rays will be significant when coherent changes in the susceptibility are large. Whilst such multi-ray effects may play a rôle in the diffraction from strong coherent optical phonons, they are unlikely to play a major part in

the diffraction from high the frequency low amplitude coherent acoustic phonons considered here, as in this latter case the changes in the susceptibility of the lattice are small. In the present analysis we continue to assume a single incident and diffracted ray, and will incorporate multiple rays in a future analysis.

2.1.1. DIFFRACTION FROM COHERENT ACOUSTIC PHONONS

Consider the situation where coherent acoustic phonons are induced within a crystal. For the sake of simplicity, we initially assume that the crystal is symmetically cut (i.e. the reciprocal lattice vector is parallel to the surface normal) in Bragg geometry, and the phonons are also propagating parallel to the surface normal. In this case, by the wavematching considerations we expect significant diffraction to occur at angular deviations of $\Delta\theta$ from the original Bragg angle, where

$$\Delta\theta = \frac{|\mathbf{q}| \tan\theta_{\mathbf{B}}}{|\mathbf{G_H}|} \tag{9}$$

Thus if the speed of sound within the crystal is v, we would expect an oscillatory signal in the time-resolved diffraction with an angular frequency ω given by

$$\omega \approx v\Delta\theta|\mathbf{G_H}| \cot\theta \tag{10}$$

Long wavelength longitudinal coherent phonons can be incorporated into the dynamical theory by noting that they alter the local Bragg angle owing to the associated straining of the lattice. If we introduce a local one-dimensional strain $\epsilon(\mathbf{r})$ into the crystal (parallel to the surface normal), then $\alpha_H(\mathbf{r})$ is given by

$$\alpha_H(\mathbf{r}) = -2\Delta\theta \sin(2\theta_B) - C\epsilon(\mathbf{r}) \tag{11}$$

where

$$C = \cos^2\phi \tan\theta_B \pm \sin\phi\cos\phi \tag{12}$$

where ϕ is the angle between the surface and the reflecting lattice plane, and the upper sign is to be used when the angle of incidence with respect to the crystal surface is $(\theta_B - \phi)$, and the lower sign when this angle is $(\theta_B + \phi)$ - i.e. we can take into account asymmetrically cut crystals. An approach such as this to the solution of the equations of dynamical diffraction in the presence of small strains was first put forward independently by Takagi and by Burgeat and Taupin.[16,17]

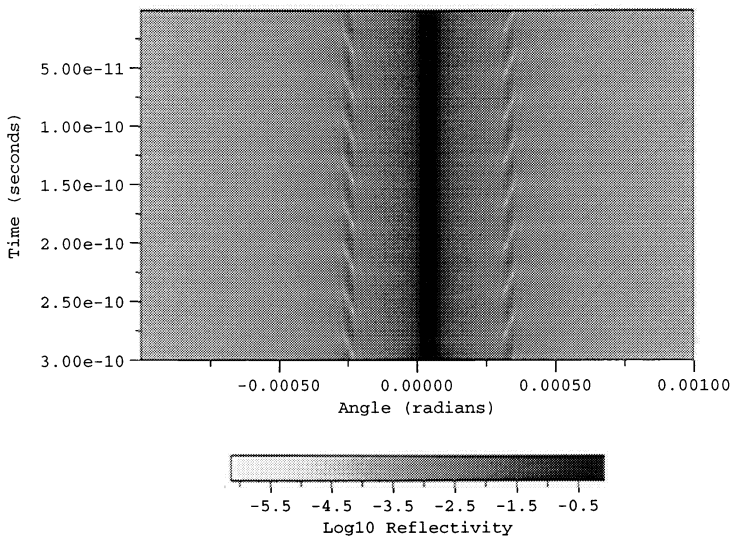

Fig. 2. Diffraction of 10 keV X-rays from the (111) plane of a GaAs symmetrically cut crystal within which an acoustic phonon of wavelength 200 nm is propagating along the direction of the surface normal. The peak strain induced by the phonon is $\pm 10^{-4}$.

In order to illustrate the above discussion, in Fig. 2 we show a simulation of the time-dependent diffraction of 10 keV X-rays from a single mode coherent phonon of peak strain amplitude $\pm 10^{-4}$ and wavelength 200 nm propagating along the surface normal in a GaAs (111) crystal. The diagram shows the logarithm of the reflectivity as a function of angular deviation from the vacuum Bragg angle. Note the offset of the main Bragg peak due to the finite d.c. component of the refractive index of the crystal. Either side of the main Bragg peak, at ± 0.316 mrad from the main peak, we see the weaker sidebands corresponding to the diffraction from the coherent phonons - this being the angular deviation predicted by equation (9). These sidebands clearly exhibit a temporal oscillation, as predicted by equation (10).

3. ACOUSTIC PHONONS: EXPERIMENTS

In real experiments involving such high frequency ($\sim$0.1 THz) acoustic phonons, a broad spectrum of coherent phonons is generated rather than a pure mode.[5,6] We outline here the recent experiments of Lindenberg and co-workers.[6] They used a Ti:Al_2O_3 150 fs, 1 kHz, 800 nm laser, synchronized to the electron bunches within the storage ring of the ALS synchrotron to irradiate an InSb single crystal. The 150 fs pulse length of the laser is much shorter than the time taken for a sound wave with speed 3900 ms^{-1} to propagate across the typical laser absorption depth of 100 nm. The laser energy is absorbed by the electrons which are excited across the band gap and heated. In the limit of instantaneous transfer of energy from the electrons to the acoustic phonons the lattice is heated at constant volume, producing an exponentially decaying pressure profile within the crystal. Subsequently the surface of the crystal starts to expand and by conservation of momentum a compression wave is launched into the bulk of the crystal. A time-dependent solution to the strain-depth profile (ignoring phonon dispersion) has been found by Thomsen and co-workers.[18] A typical strain-depth profile given such assumptions for the irradiated InSb is shown in Fig. 3. This strain profile may be thought of as a superposition of coherent phonons, with wavevectors peaked around an inverse of the laser penetration depth.

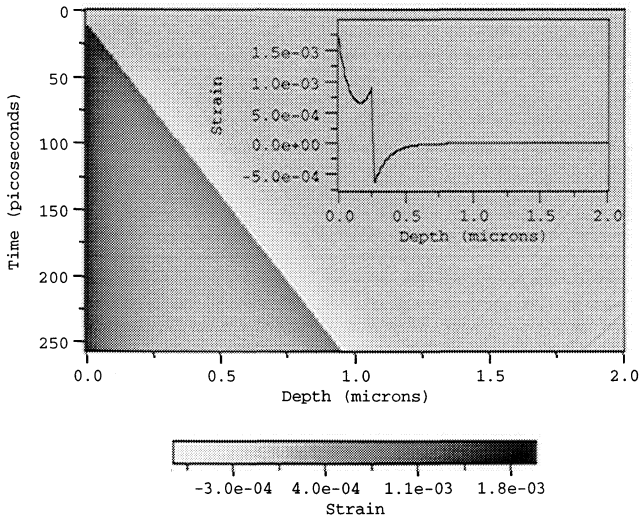

Fig. 3. Strain as a function of depth within the InSb crystal assuming instantaneous heating with a $1/e$ depth of 100 nm. The lattice temperature at the crystal surface is taken to be just below the melting point. Diffusion, finite electron-phonon coupling time and phonon dispersion have been ignored. The inset shows a lineout of the strain-depth profile taken at 75 ps.

After the strain pulse was launched into the InSb crystal, X-rays emitted by the synchronised electron bunches of wavelength 2.4$\mathring{A}$ and spectral bandwidth 1 m$\mathring{A}$ were diffracted from the crystal and recorded on a streak camera. The streak camera was triggered by the same laser using a photoconducting switch. The data were averaged over 60,000 shots. To better match the penetration depths of the laser and the X-rays the crystal was cut asymmetrically

such that the X-rays reflecting from the (111) planes left the crystal at a grazing angle of 3^0. Fig. 4 shows the computed logarithm of the time-dependent reflectivity assuming the strain profile given in Fig. 3. Note that if we collect data at a particular angular position away from the original Bragg angle we will once more observe temporal oscillations in the X-ray reflectivity.

Fig. 5 shows the experimentally observed time-dependent diffracted intensity measure at +40 arc sec from the Bragg peak. Alongside the data we show the calculated intensity. However, we emphasise that to get a good match between the experimental and computed profiles it is necessary to modify the analytical solution to the strain-depth profile given by Thomsen and co-workers.[18] In particular the first 10 ps cannot be modelled without inclusion of a fast term in the strain generation, whilst the long-time behaviour cannot be modelled without a slower developing term which tends to smooth the interface between the compressed and rarefied regions of the crystal. The physical mechanisms that give rise to such behaviours may be related to the deformation-potential generated stress and the finite electron-phonon coupling time. We might also expect similar effects due to phonon dispersion, which has been ignored in these calculations.

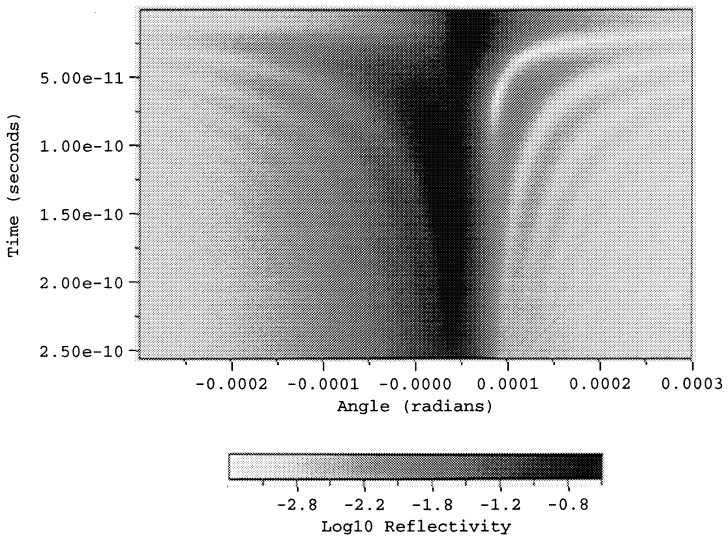

Fig. 4. Simulated time-dependent X-ray diffraction for 2.4Å radiation diffracting from the asymmetric InSb crystal described in the text, assuming the strain history plotted in Fig. 3.

The simulation presented in Fig. 5 has also taken into account the finite bandwidth of the X-ray source (as opposed to the simulation shown in Fig. 4 which is a rocking curve - i.e. it assumes perfectly monochromatic radiation incident upon the source). Such source bandwidth effects reduce the visibility of the temporal oscillations, as they correspond to a finite angular resolution according to

$$\Delta\theta_{bw} = \frac{\tan\theta\Delta\lambda_{eff}}{\lambda} \tag{13}$$

where $\Delta\lambda_{eff}$ is the effective bandwidth.

3.1. ACOUSTIC PHONONS: INCREASING THE DISPERSION

As noted above, source bandwidth issues are a potential problem in observing diffraction from coherent phonons. When using synchrotron sources, which are normally pre-monochromated before the diffracting crystal of interest, one should ideally operate in the mode where the diffracting planes of the sample crystal are parallel to those of the final crystal of the monochromator. When the lattice spacings of these two diffracting crystals are well matched the resultant effective bandwidth is then limited by the rocking curve width of the monochromator. In addition (and in contrast to the experiment described above) there are certain advantages to diffracting from asymmetrically-cut

crystals, but with the X-ray beam *incident* at grazing angles. The reason that this is advantageous can be seen by considering equations (11) and (12). If the angular resolution of the experiment is limited by the effective bandwidth, as in equation (13), then it is good practice to make the dispersion of the system as high as possible. That is to say, it is of benefit to ensure that a given strain within the crystal corresponds to a large angular deflection - i.e. we need to make the factor C of equations (11) and (12) as large as possible. For this to occur, we need to add rather than substract the two terms in equation (12), and thus we need the angle of incidence to be grazing.

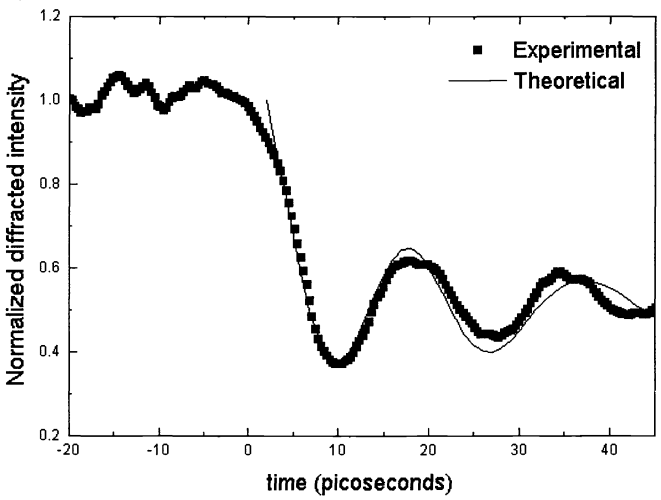

Fig. 5. Experimental and simulated time-dependent X-ray diffraction for 2.4$\AA$ radiation diffracting from the asymmetric InSb crystal described in the text, at +40 arc sec from the main Bragg peak.

The underlying physics of this increase in dispersion is that when we introduce a one-dimensional strain into the crystal the planes not only change in spacing, but they also rotate. If the X-rays are incident at grazing angles these two effects have the same sign, whereas if the X-rays leave at grazing incidence they tend to cancel out, and the rocking curve of the sample crystal becomes narrow, and there is only a small angular deflection for a given value of strain within the crystal. Note however that although such approach increases the dispersion, it brings withit the associated problem that the footprint of the X-ray beam on the crystal surface is increased, and thus the footprint of the laser irradiating the crystal (which should be as close to co-linear with the X-ray beam as possible to minimise the temporal smearing) is also increased: thus higher laser energies are required for a given irradiance.

4. OPTICAL PHONONS

Whilst acoustic phonons alter the local Bragg angle, coherent optical phonons alter the local complex susceptibility of the lattice, as they correspond to a coherent movement of atoms within the unit cell thus changing the local structure factors. As with acoustic phonons, coherent optical phonons can be generated within a medium by irradiating it with a femtosecond laser pulse, with the phonons being induced by either the so-called displacive or Raman mechanisms. Conventionally, such coherent phonons have been diagnosed by registering the effect of the phonon field on the optical properties of the medium, but in principle they should also be observable in X-ray diffraction. However, several difficulties remain if they are to be observed experimentally by such means, and perhaps utilised for novel X-ray optics (see section 5). Firstly, it is necessary to find crystals and reflections for which the atomic motions associated with the phonons correspond to relatively large changes in structure factors; secondly, it would be useful if such modes could be induced within the crystal on distances comparable with the X-ray absorption and/or extinction depth; and finally optical phonons generally have far higher frequencies than their acoustic counterparts, and thus

significantly improved temporal resolution would aid in their diagnosis. Indeed, it could be in this area where the ultra-short femtosecond durations of the FEL pulse could be particularly advantageous.

4.1. SIMULATION OF DIFFRACTION FROM OPTICAL MODES IN BISMUTH

To date, to our knowledge no successful X-ray diffraction experiments from coherent optical phonons have been prosecuted. Thus we restrict ourselves to the results of our initial simulations of such effects. As an example of the effects of optical phonons on the diffraction signal, we present below a preliminary analysis of the diffraction of 10 keV X-rays from a single crystal of Bismuth. Bismuth has been chosen for a number of reasons. Firstly, several experiments have previously been performed on this material, and the effects of the phonons on the optical reflectivity noted.[19] Secondly, a theoretical study of the phonon generation process has given rise to reasonable estimates of both the nature and amplitude of the excited phonon modes, thus enabling us to make an informed evaluation of the influence of such modes on the X-ray susceptibilities, and hence diffraction properties. Finally, as shown below, we find that the physical structure of Bismuth is such that relatively small amplitude phonons can potentially produce large changes in the X-ray reflectivity for a judicial choice of X-ray reflections, though the short laser absorption depths present difficulties.

Bismuth possesses a trigonal primitive unit cell, containing two atoms at $(\pm u, \pm u, \pm u)$, where under ambient conditions $u = 0.237$. The conventional unit cell is hexagonal (with unit cell parameters $a = 4.546\mathring{A}$, $c = 11.862\mathring{A}$), containing 3 lattice points and 6 atoms, again with a basis of two atoms at $(0, 0, \pm u)$. Irradiation by the short pulse laser excites optical phonons via the displacive mechanism, thereby setting up an oscillation of the A1 so-called breathing mode in which the two atoms within the basis oscillate symmetrically - that is to say the coordinate u becomes time and space dependent and, for a pure phonon travelling in the $+x$ direction with freqency ω and wavevector q can be written

$$u(t) = u_0 + A\exp[i(\omega t - qx)]\exp(-\gamma t) \tag{14}$$

where γ is related to the damping of the mode. For the A1 mode, ω is found to be 2.75 THz,[19] and γ^{-1} is of order 3.8 psec.[20]

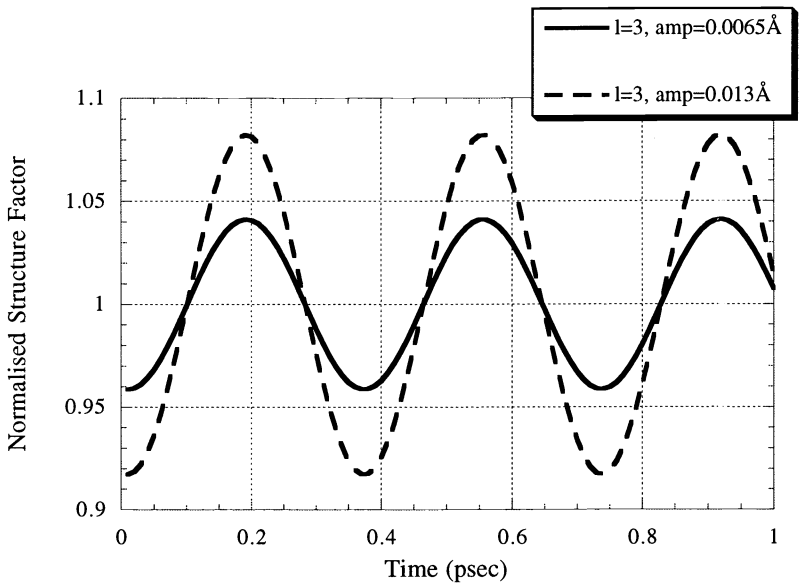

Fig. 6. Time-dependent relative structure factor for diffraction from the (0,0,3) plane of Bismuth in the presence of coherent optical phonons of amplitude $0.0065\mathring{A}$ and $0.013\mathring{A}$.

It is estimated that the amplitude of the displacement of the atoms within the unit cell can reach of order $0.013\mathring{A}$ when approximately 3×10^{20} cm^{-3} electrons are transferred to an excited band (corresponding to approximately 2% of the electrons).[19] Given the length of the c axis, this amplitude then corresponds to a value of A in equation (14) of only 1.1×10^{-3}. Although this is an extremely small displacement, it can have a relatively large effect on the structure factor of the crystal for certain reflections. For reflections with low values of Miller indices (where the reflectivity is not greatly compromised by the Debye-Waller effect at room temperature) the influence of the atomic displacements is greatest for the $(0,0,3)$ reflection. Note that for this reflection the structure would vanish (assuming spherically symmetric atomic form factors) if $u = \pm 0.25$: the ambient position of the atoms at $u = \pm 0.237$ is sufficiently close to this position to give rise to significant relative changes in the structure factor for the expected small atomic displacements. For the $q = 0$ A1 mode, the time-dependent structure factor, $S(t)$, normalised to the structure factor under ambient conditions for the $(0,0,l)$ reflection is given by

$$\frac{S(t)}{S(0)} = \frac{cos[2\pi l u(t)]}{cos[2\pi l u_0]} \tag{15}$$

and we plot this for the $(0,0,3)$ reflections for two values of the amplitude (neglecting damping) in Fig. 6. Note the large relative change in the structure factor ($\pm 8\%$) for the small fractional changes in atomic positions.

Pure single mode optical phonons of wavevector $\mathbf{q}$ also produce sidebands. However, in practice the observation of coherent optical phonons in Bismuth is likely to be hampered by the extremely small laser absorption depths. According to the parameters supplied by Zeiger and co-workers, the absorption depth for the 800 nm laser in Bismuth is only of order 12.5 nm;[19] the X-ray penetration depth is likely to be much larger than this, and thus any modulation in the X-rays diffracted from the sample is likely to be swamped by the signal from the unperturbed bulk, and indeed our initial calculations confirm this.

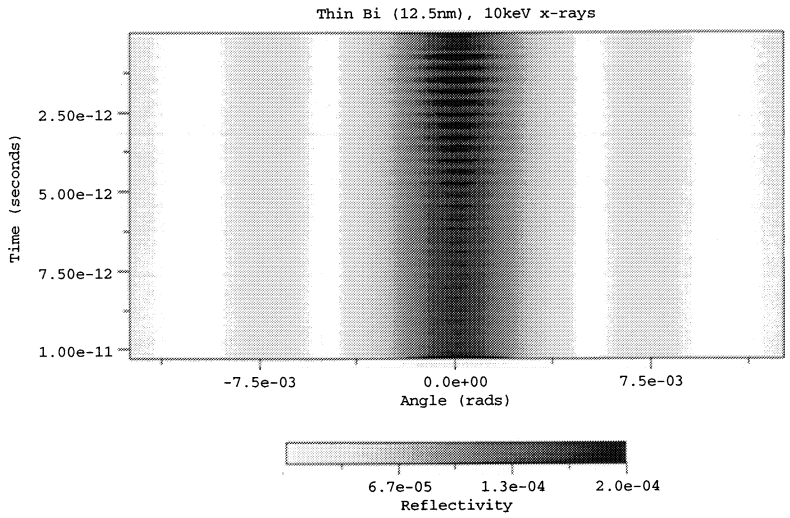

Fig. 7. Time-dependent diffraction of 10 keV X-rays from the (0,0,3) plane of a 12.5 nm thick Bismuth crystal in the presence of coherent optical phonons of amplitude $0.013\mathring{A}$ with a decay depth within the crystal of 12.5 nm.

Given the short absorption depth of the laser within Bi, we have simulated the diffraction from a thin single crystal in order to increase the contrast of the temporal oscillations. Fig. 7 shows the simulated diffraction of 10 keV X-rays from a 12.5 nm thick single crystal of Bi, assuming that the phonons do not propagate (the group velocity of

the optical phonons is small). The initial amplitude of the phonons is assumed to decay with the same decay length as the intensity of the laser. The temporal oscillations in the reflectivity of the peak can clearly be seen, although the peak reflectivity of the reflection is low, and its overall angular width large, owing to the small and finite thickness of the crystal. Ideally for the study of optical phonons we need to identify crystals where the absorption of the laser radiation is relatively low, yet phonons can still be excited which can radically alter the X-ray structure factors. Crystals with optical modes excited by Raman processes may exhibit such characteristics.

5. THE PHONON-BRAGG SWITCH

Bucksbaum and Merlin have recently suggested that coherent optical phonons may be used to generate a Phonon-Bragg (PB) switch.[9] The basic concept is shown in schematic form in Fig. 8. Two femtosecond laser beams with wavevectors $\mathbf{k_1^1}$ and $\mathbf{k_2^1}$ are incident upon the crystal from almost opposite directions, with angles of incidence θ_i. It is proposed that these set up a superlattice of optical phonons with a period of $2\pi/q = \lambda/(2n)$, where $\mathbf{q} = \mathbf{k_1^1} - \mathbf{k_2^1}$ and λ is the wavelength of the laser, and n the refractive index of the crystal. Note that the wavevector of the phonons is perpendicular to the surface normal. Bucksbaum and Merlin show that the coherent phonon superlattice leads to a new series of Bragg peaks given by the phase matching condition $\Delta\mathbf{k} = \mathbf{G_H} \pm \mathbf{q}$, similar to the manner in which X-ray diffraction from surface acoustic phonons at MHz frequencies can introduce additional Bragg peaks.[21,22] However, they propose that the duration of this superlattice can be controlled by turning off the oscillation coherently by the application of a second laser pulse (see Fig. 8) half a phonon period after the first. For a GaAs optical phonon this would result in an X-ray pulse of order 100 fs duration.

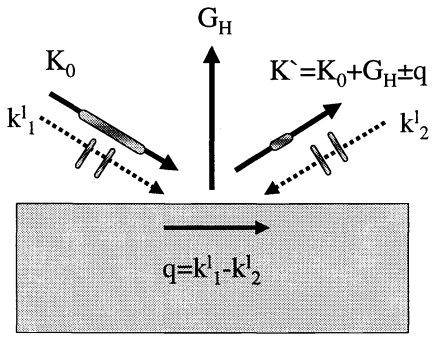

Fig. 8. A schematic diagram of the Phonon-Bragg Switch. Two laser beams of wavevectors $\mathbf{k_1^1}$ and $\mathbf{k_2^1}$ are incident upon the crystal from almost opposite directions, with angles of incidence θ_i. They set up a superlattice of optical phonons with a period of $2\pi/q = \lambda/(2n)$, where $\mathbf{q} = \mathbf{k_1^1} - \mathbf{k_2^1}$, from which the X-rays scatter into new angles satisfying $\Delta\mathbf{k} = \mathbf{G_H} \pm \mathbf{q}$

6. FEMTOSECOND DYNAMICAL DIFFRACTION

In all of the simulations presented thus far we have ignored the derivative with respect to time in equations (6) and (7): that is to say we have assumed that the X-ray pulse length and/or the changes in crystal properties were long compared with the time taken for the X-rays to traverse an extinction depth. Such an approximation is likely to be valid, even for the 300 fs period of the optical phonons in Bismuth, However, as the duration of the X-ray pulse is reduced still further (i.e. to the femtosecond levels that may be achievable with FELs), the finite duration of the pulse itself may be of import, as will alterations in the crystal structure on such timescales. To illustrate the point, we note that the duration of a diffracted X-ray pulse from a thick single crystal is ultimately limited by the extinction depth traversal time. Fig. 9 shows the time-dependent rocking curve as a function of dimensionless time, T, and angle, y, for a beam suddenly switched on at time $T = 0$. The properties of the crystal are defined in terms of Zachariasen's dimensionless units k and g where

$$g = \frac{\psi_0''(\mathbf{r}, 0)}{K|\psi_H'(\mathbf{r}, 0)|} \tag{16}$$

$$k = \frac{\psi''_H(\mathbf{r}, 0)}{\psi'_H(\mathbf{r}, 0)} \tag{17}$$

where $K = 1$ for normal polarisation, and $K = |\cos 2\theta_B|$ for parallel polarisation. Zachariasen's unit of dimensionless angle is

$$\frac{y = \psi'_0(\mathbf{r}, 0) + \frac{1}{2}\alpha_H}{K|\psi'_H(\mathbf{r}, 0)|} \tag{18}$$

We further define units of dimensionless time as

$$T = \frac{c\pi K|\psi'_H(\mathbf{r}, 0)|t}{\sin^2\theta\lambda} \tag{19}$$

In these units an X-ray traverses an extinction depth in unit dimensionless time. We note that the angularly integrated reflectivity asymptotes to its steady state value at approximately $T = 2$, as would be expected by the time taken for a beam to enter and leave the crystal. That said, narrow angular features within the rocking curve take longer to reach the steady state.

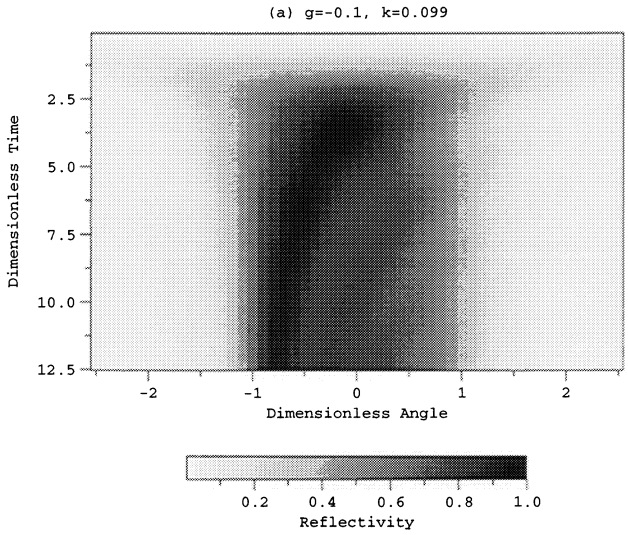

Fig. 9. Rocking curve as a function of time for X-rays switched on at time $T = 0$. The simulated reflectivity is plotted as a function of dimensionless angle and time, and the characteristics of the crystal are defined in terms of the dimensionless parameters $k = 0.099$ and $g = -0.1$ (see text for definition of dimensionless variables).

7. SUMMARY AND CONCLUSIONS

In summary, the opportunities afforded by the capacity to perform X-ray diffraction experiments on femtosecond timescales presents new opportunities for experiments in widely ranging fields of science. Whilst femtosecond FEL based sources may be some time away, many experiments are starting to be performed with existing sources. We have summarised here several novel experiments and concepts in the field of coherent phonon physics, illustrating how such phonons may be detected with time-resolved diffraction, and how, in principle, fast X-ray optics such as the Phonon-Bragg switch may be developed.

REFERENCES

1. V. Srajer, T. Tsu-Yi, T. Ursby, C. Pradervand, R. Zhong, S. I. Adachi, W. Schildkamp, D. Bourgeois, M. Wulff, and K. Moffat, "Photolysis of the carbon monoxide complex of myoglobin: nanosecond time-resolved crystallography," *Science* **274**, pp. 1726–1729, 1996.

2. B. Perman, V. Srajer, R. Zhong, T. Tsu-Yi, C. Pradervand, T. Ursby, D. Bourgeois, F. Schotte, M. Wulff, R. Kort, K. Hellingwerf, and K. Moffat, "Energy transduction on the nanosecond timescale: early structural events in a xanthopsin photocycle," *Science* **279**, pp. 1946–1950, 1998.
3. J. Larsson, P. A. Heimann, A. M. Lindenberg, P. J. Schuck, P. H. Bucksbaum, R. W. Lee, H. A. Padmore, J. S. Wark, and R. W. Falcone, "Ultrafast structural changes measured by time-resolved x-ray diffraction," *Appl. Phys. A* **66**, pp. 587–591, 1998.
4. C. Rischel, A. Rousse, I. Uschmann, P. A. Albouy, J. P. Geindre, P. Audebert, J. C. Gauthier, E. Forster, J. L. Martin, and A. Antonetti, "Femtosecond time-resolved x-ray diffraction from laser-heated organic films," *Nature* **390**, pp. 490–492, 1997.
5. C. Rose-Petruck, R. Jimenez, T. Guo, A. Cavalleri, C. W. Siders, F. Raksi, J. A. Squier, B. C. Walker, K. R. Wilson, and C. P. J. Barty, "Picosecond-milliangstrom lattice dynamics measured by ultrafast x-ray diffraction," *Nature* **398**, pp. 310–312, 1999.
6. A. M. Lindenberg, I. Kang, S. L. Johnson, T. Missalla, P. A. Heimann, Z. Chang, J. Larsson, P. H. Bucksbaum, H. C. Kapteyn, H. A. Padmore, R. W. Lee, J. S. Wark, and R. W. Falcone, "Time-resolved x-ray diffraction from coherent phonons during a laser-induced phase transition," *Phys. Rev. Lett.* **84**, pp. 111–114, 2000.
7. R. W. Schoenlein, W. P. Leemans, A. H. Chin, P. Volfbeyn, T. E. Glover, P. Balling, M. Zolotorev, K. J. Kim, S. Chattopadhyay, and C. V. Shank, "Femtosecond x-ray pulses at 0.4 angstrom generated by 90-degrees thomson scattering - a tool for probing the structural dynamics of materials," *Science* **274**, pp. 236–238, 1996.
8. C. W. Siders, A. Cavalleri, K. Sokolowskitinten, C. Toth, T. Guo, M. Kammler, M. H. Vonhoegen, K. R. Wilson, D. Vonderlinde, and C. P. J. Barty, "Detection of nonthermal melting by ultrafast x-ray diffraction," *Science* **286**, pp. 1340–1342, 1999.
9. P. H. Bucksbaum and R. Merlin, "The phonon bragg switch - a proposal to generate subpicosecond x-ray pulses," *Solid State Commun.* **111**, pp. 535–539, 1999.
10. W. H. Zachariasen, *The Theory of X-Ray Diffraction in Crystals*, Wiley, New York, 1945 (reprinted by Dover Publications in 1994).
11. J. S. Wark and H. He, "Subpicosecond x-ray diffraction," *Laser and Particle Beams* **12**, pp. 507–513, 1994.
12. J. S. Wark and R. W. Lee, "Simulations of femtosecond x-ray diffraction from unperturbed and rapidly heated single crystals," *J. Appl. Crystallogr.* **32**, pp. 692–703, 1999.
13. F. N. Chukhovskii and E. Forster, "Time-dependent x-ray bragg diffraction," *Acta Crystallogr. A* **51**, pp. 668–672, 1995.
14. S. Sytova, "X-ray diffraction by time-dependent deformed crystals: Theoretical model and numerical analysis," LANL Physics Preprints arXiv:physics/9901033, 1999.
15. C. R. Wie, T. A. Tombrello, and J. T. Vreeland, "Dynamical x-ray diffraction from nonuniform crystalline films: Application to x-ray rocking curve analysis," *J. Appl. Phys.* **59**, pp. 3743–3746, 1986.
16. S. Takagi, "Dynamical theory of diffraction applicable to crystals with any kind of small distortion," *Acta Crystallogr.* **15**, pp. 1311–1311, 1962.
17. J. Burgeat and D. Taupin, "Application de la théorie dynamique de la diffraction x à l'étude de la diffusion du bore et du phosphore dans les cristaux de silicium," *Acta Crystallogr. A* **24**, pp. 99–102, 1968.
18. C. Thomsen, H. T. Grahn, H. J. Maris, and J. Tauc, "Surface generation and detection of phonons by picosecond light pulses," *Phys. Rev. B* **34**, pp. 4129–4138, 1986.
19. H. J. Zeiger, J. Vidal, T. K. Cheng, E. P. Ippen, G. Dresselhaus, and M. S. Dresselhaus, "Theory for displacive excitation of coherent phonons," *Phys. Rev. B* **45**, pp. 768–778, 1993.
20. M. Hase, K. Mizoguchi, H. Harima, S. ichi Nakashima, and K. Sakai, "Dynamics of coherent phonons in bismuth generated by ultrashort laser pulses," *Phys. Rev. B* **58**, pp. 5448–5452, 1998.
21. S. D. LeRoux, R. Colella, and R. Bray, "X-ray diffraction studies of acoustoelectrically amplified phonon beams," *Phys. Rev. Lett.* **35**, pp. 230–234, 1975.
22. R. Tucoulou, D. V. Roshchupkin, O. Mathon, I. A. Schelokov, M. Brunel, E. Ziegler, and C. Morawe, "High-frequency x-ray beam chopper based on diffraction by surface acoustic waves," *J. Synchrotron Rad.* **5**, pp. 1357–1362, 1998.